The one-half spin free Larmor and parametrically induced Rabi precessions simulated with two coupled pendula

Valentin Leroy, Jean-Claude Bacri, Thierry Hocquet, Martin Devaud

The one-half spin free Larmor and parametrically induced Rabi precessions simulated with two coupled pendula

V Leroy, J-C Bacri, T Hocquet and M Devaud

Laboratoire Matière et Systèmes complexes (MSC),
UMR 7057 (CNRS) and Université Denis Diderot,
10 rue Alice Domon et Léonie Duquet, 75013 PARIS

E-mail: thierry.hocquet@upmc.fr

Abstract. It was already shown that, with a simplest classical device, namely two coupled pendula, one can simulate the movement of a free quantum two-level system, as for instance a one-half spin in a static magnetic field. We now show that, with a hardly more sophisticated device, one can simulate the latter system undergoing a sinusoidal perturbation. We present an experimental mechanical illustration of the transition of the system between its two eigenstates, known as the Rabi precession. Abstract theoretical concepts of absorption and stimulated emission of energy are thus provided with an intuitive support.

PACS numbers: 45.20.-d, 45.20.Jj, 45.05.+x

1. Introduction

In the course of the undergraduate level academic progress, the students' first contact with Quantum Mechanics (QM) is always a rather puzzling experience. *Per se*, this perturbation is neither unique nor pathological: facing a new concept, like for instance the non Euclidian metrics of space-time in Special Relativity, is not surprisingly disturbing, and every major step in our understanding the world invariably began with a disturbance in our preexisting conceptions. But the unease of students faced with their QM primers is a bit particular in that it has an entangled twofold origin: the novelty of *both* the physical concepts and the mathematical Hamiltonian formalism. The upshot of this is that it is rather difficult (at least at the undergraduate level) to tell a purely quantum effect from a fairly classical one dressed in QM guise. Conversely, it is possible to simulate quantum behaviours with purely classical physics and devices. Such simulations are interesting from a pedagogical point of view: students are gradually and painlessly won over by quantum ideas and vocabulary. Moreover, they are provided with what is most lacking for beginners in QM: an intuitive support.

It is the aim of the present paper to show how a typically quantum process, namely a one-half spin undergoing the so-called Rabi precession, can be simulated, both theoretically and experimentally, with a most simple classical system: two coupled pendula.

In a foregoing paper [1], we have already shown that the *free* movement of such a two-pendulum system is, under certain conditions that we have specified at some

length, formally analogous to a one-half spin precessing in a static magnetic field (Larmor precession). In the present paper, we go a step further and show that an *ad hoc* parametric excitation of the system – a small sinusoidal modulation of the length of one of the coupled pendula under the circumstances – enables us to observe transitions between the two eigenmodes of the free two-pendulum oscillator. These transitions (as for any sinusoidally perturbed two-level system in QM) can all the same be regarded as the Rabi precession undergone by a one-half fictitious spin submitted to both a static and a rotating magnetic field.

The above topics may concern the same readership as does [1], namely undergraduate level students as well as their teachers. An easy understanding of these topics requires, to our opinion, a good mastery of the content and results of [1]. We consequently suggest a preliminary study of this foregoing paper, the notations of which have been carefully conserved in the present article. The readers who would have followed this suggestion may then jump directly to section 3. Nevertheless, for those readers who prefer an all-in-one-block presentation, we have condensed the material of [1] in section 2, which sets this paper self-consistent. The latter is therefore organized as follows.

Section 2 is devoted to a wide recall (although with a slightly different presentation) of the main results of [1]. In section 3, we deal with the problem of the parametric excitation of the two-pendulum system, first in the general case (subsection 3.1), then in the quasi-degeneracy limit (subsection 3.2). In the latter limit, we carefully distinguish the representation in the Hilbert space (3.2.1) and that in the Larmor space (3.2.2). In section 4, we focus on the Rabi precession. We begin with our experimental device (subsection 4.1). We then carry out the calculation in the Hilbert space (subsection 4.2) and present our experiment (subsection 4.3). Next we resume the calculations in the Larmor space (subsection 4.4) and we draw up an energy balance of the process (subsection 4.5). We conclude this paper in section 5.

2. The free two-pendulum system

2.1. The general case

Let us consider two pendula than can rotate freely around some horizontal axis (A). The natural dynamic variables of the system are the angles θ_1, θ_2 made by the pendula with the vertical, so that $\theta_1 = \theta_2 = 0$ is the equilibrium position. Let J_1 and ℓ_1 (resp. J_2 and ℓ_2) be the inertia momentum with respect to axis (A) and the {centre of mass to axis (A)} distance of pendulum 1 (resp. 2). The pendula are coupled through a torsion wire with angular stiffness C, and have a common total mass M. This device is sketched in figure 1.

In the absence of any external torque, the dissipation-free equations of motion read

$$\begin{aligned} J_1\ddot{\theta}_1 &= -Mg\ell_1 \sin\theta_1 - C(\theta_1 - \theta_2), \\ J_2\ddot{\theta}_2 &= -Mg\ell_2 \sin\theta_2 - C(\theta_2 - \theta_1), \end{aligned} \tag{1}$$

where g is the gravity acceleration. We shall henceforth assume that the oscillation amplitudes are small and linearize $\sin\theta_1$ (resp. $\sin\theta_2$) in θ_1 (resp. θ_2).

Introducing the standard dynamical variables ($k = 1, 2$)

$$q_k = \sqrt{J_k}\theta_k, \tag{2a}$$

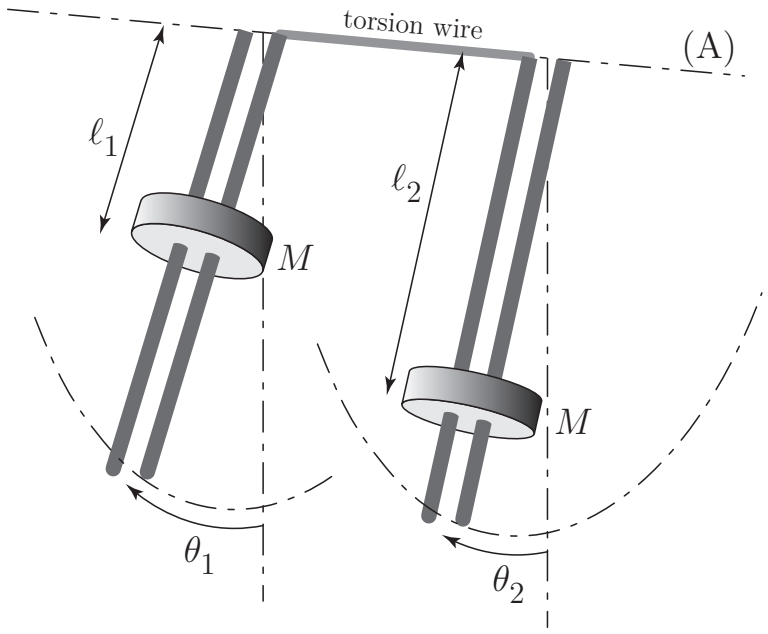

Figure 1. Experimental device. Both pendula can rotate freely around axis (A). They are coupled through a torsion wire. Angles θ_1 and θ_2 are measured by means of two potentiometers connected to a numerical oscilloscope.

setting

$$\omega_k^2 = \frac{Mg\ell_k + C}{J_k}, \tag{2b}$$

and defining the dimensionless coupling constant κ by

$$\frac{C}{\sqrt{J_1 J_2}} = \kappa\,\omega_1\omega_2 \quad \rightsquigarrow \quad \kappa = \frac{C}{\sqrt{(Mg\ell_1 + C)(Mg\ell_2 + C)}} \leqslant 1, \tag{2c}$$

the equations of motion (1) read

$$\ddot{q} + B^2 q = 0, \tag{3}$$

where

$$q = \begin{pmatrix} q_1 \\ q_2 \end{pmatrix} \quad \text{and} \quad B^2 = \begin{pmatrix} \omega_1^2 & -\kappa\,\omega_1\omega_2 \\ -\kappa\,\omega_1\omega_2 & \omega_2^2 \end{pmatrix}. \tag{4}$$

The above equation (3) can be derived from the Lagrangian

$$L = \frac{1}{2}({}^t\dot{q}\dot{q} - {}^t q B^2 q) \tag{5a}$$

(superscript ^{t} indicating matricial transposition) or from the Hamiltonian

$$H = \frac{1}{2}({}^t p p + {}^t q B^2 q), \tag{5b}$$

where $p = \begin{pmatrix} p_1 \\ p_2 \end{pmatrix} = \dfrac{\partial L}{\partial \dot{q}}$ are the conjugate momenta of variables q.

Unless the coupling constant κ is zero, matrix B^2 is nondiagonal (see (4)) and the dynamic variables q_1 and q_2 are coupled together. In order to find a pair of uncoupled dynamic variables, the standard procedure consits in diagonalizing matrix B^2, that is to find a passage matrix P_e such that

$$P_e^{-1}B^2P_e = \begin{pmatrix} \omega_+^2 & 0 \\ 0 & \omega_-^2 \end{pmatrix}. \tag{6a}$$

It is noteworthy that, since matrix B^2 is *real* and *symmetrical*, it is possible to get an *orthogonal* passage matrix P_e, *i.e.* to have $P_e^{-1} = {}^tP_e$. We shall henceforth assume that P_e is orthogonal and set

$$P_e = \begin{pmatrix} \cos\frac{\phi_e}{2} & \sin\frac{\phi_e}{2} \\ -\sin\frac{\phi_e}{2} & \cos\frac{\phi_e}{2} \end{pmatrix}. \tag{6b}$$

Then, introducing the so-called normal variables (φ_+, φ_-) defined by

$$q = P_e\varphi \quad \text{with} \quad \varphi = \begin{pmatrix} \varphi_+ \\ \varphi_- \end{pmatrix}, \tag{7}$$

the matricial equation (3) is turned into the following set of two uncoupled equations:

$$\ddot{\varphi} + P_e^{-1}B^2P_e\varphi = 0 \quad \rightsquigarrow \quad \left| \begin{array}{l} \ddot{\varphi}_+ + \omega_+^2\varphi_+ = 0 \\ \ddot{\varphi}_- + \omega_-^2\varphi_- = 0 \end{array} \right. . \tag{8}$$

Not surprisingly, eqs. (8) can be derived from Lagrangian (5a) which reads, using the normal variables

$$\begin{aligned} L &= \frac{1}{2}\left({}^t\dot{\varphi}{}^tP_eP_e\dot{\varphi} - {}^t\varphi{}^tP_eB^2P_e\varphi\right) \\ &= \frac{1}{2}(\dot{\varphi}_+^2 - \omega_+^2\varphi_+^2) + \frac{1}{2}(\dot{\varphi}_-^2 - \omega_-^2\varphi_-^2), \end{aligned} \tag{9}$$

i.e. as the sum of two independent HO1 lagrangians. Consequently, $\pi = \begin{pmatrix} \pi_+ \\ \pi_- \end{pmatrix}$ standing for the conjugate momenta of φ, one has:

$$\pi = \frac{\partial L}{\partial\dot{\varphi}} = \dot{\varphi} = P_e^{-1}\dot{q} = P_e^{-1}p \quad \rightsquigarrow \quad p = P_e\pi, \tag{10}$$

so that Hamiltonian (5b) reads

$$H = \frac{1}{2}(\pi_+^2 + \omega_+^2\varphi_+^2) + \frac{1}{2}(\pi_-^2 + \omega_-^2\varphi_-^2), \tag{11}$$

hence equations (8) again using Hamiton's formalism.

As will appear in the following, it is interesting to note what turns out when use is made of the Glauber‡ variables (α_1, α_2) of the pendula to express Hamiltonian (5b). Defining

$$\alpha_k = \frac{1}{\sqrt{2\hbar}}\left(\sqrt{\omega_k}q_k + \frac{\mathrm{i}}{\sqrt{\omega_k}}p_k\right) \qquad (k = 1, 2), \tag{12a}$$

one readily obtains:

$$H = \hbar\omega_1|\alpha_1|^2 + \hbar\omega_2|\alpha_2|^2 - \kappa\frac{\hbar}{2}\sqrt{\omega_1\omega_2}(\alpha_1 + \alpha_1^*)(\alpha_2 + \alpha_2^*). \tag{12b}$$

‡ The Glauber variables are used throughout [1]. Moreover, they are introduced in subsection (2.1) of our foregoing study [2]. For a more complete intoduction to the Glauber formalism, see [3], [4], [5] or [6].

From the above Hamiltonian (12*b*), and considering the Poisson's brackets

$$\{\alpha_k, \alpha_{k'}\} = \{\alpha_k^*, \alpha_{k'}^*\} = 0; \quad \{\alpha_k, \alpha_{k'}^*\} = \frac{1}{\mathrm{i}\hbar}\delta_{kk'}, \tag{13}$$

one derives the following equations of motion:

$$\dot{\alpha}_1 = \{\alpha_1, H\} = -\mathrm{i}\omega_1\alpha_1 + \mathrm{i}\frac{\kappa}{2}\sqrt{\omega_1\omega_2}(\alpha_2 + \alpha_2^*), \tag{14a}$$

$$\dot{\alpha}_2 = \{\alpha_2, H\} = -\mathrm{i}\omega_2\alpha_2 + \mathrm{i}\frac{\kappa}{2}\sqrt{\omega_1\omega_2}(\alpha_1 + \alpha_1^*). \tag{14b}$$

It is interesting too to introduce the eigenmodes' proper Glauber variables, *i.e.* the Glauber variables associated with the normal variables set $\{\varphi, \pi\}$. Defining

$$\alpha_\pm = \frac{1}{\sqrt{2\hbar}}\left(\sqrt{\omega_\pm}\varphi_\pm + \frac{\mathrm{i}}{\sqrt{\omega_\pm}}\pi_\pm\right), \tag{15a}$$

one easily derives from equation (11)

$$H = \hbar\omega_+|\alpha_+|^2 + \hbar\omega_-|\alpha_-|^2. \tag{15b}$$

Using again Poisson's relations (13), with k and k' now standing for $+$ or $-$ (instead of 1 or 2), one consequently finds

$$\dot{\alpha}_\pm = \{\alpha_\pm, H\} = -\mathrm{i}\omega_\pm\alpha_\pm \quad \rightsquigarrow \quad \alpha_\pm(t) = \alpha_\pm(0)\,\mathrm{e}^{-\mathrm{i}\omega_\pm t}. \tag{16}$$

As a consequence, the semiclassical quanta numbers $|\alpha_+|^2$ and $|\alpha_-|^2$ are *separately* constants of motion.

It is noteworthy that, although equations (14) and (16) are perfectly equivalent, passing from the former to the latter is not straightforward at all. This is due to the fact that, in the general case of the present subsection, there is no simple relation between (α_1, α_2) and (α_+, α_-). Note for instance that, contrary to equations (16), equations (14) *are not* linear, due to the presence of the starred terms on their right-hand sides. We shall now recall in the following subsection how these difficulties vanish in the quasi-degeneracy limit.

2.2. The quasi-degeneracy limit

Substantial simplifications of the two-degree of freedom problem occur when eigen angular frequencies ω_+ and ω_- of the two-pendulum system are close to each other, and the motion equation of the HO2 is then "Schrödinger-like". Moreover, the corresponding movement can be described using the Schwinger-Larmor geometrical representation. Let us briefly sketch these points.

2.2.1. New simplifications and Hilbert space Let us set

$$\omega_0 = \frac{\omega_1 + \omega_2}{2}, \qquad \Delta = \omega_1 - \omega_2, \tag{17}$$

and assume that *simultaneously*

$$|\Delta| \ll \omega_0 \quad \text{(small detuning)} \quad \text{and} \quad \kappa \ll 1 \quad \text{(small coupling)}. \tag{18}$$

Allowing from the above conditions (18), it is easy to check that one has also $|\omega_+ - \omega_-| \ll \omega_0$, hence the "quasi-degeneracy" term we choose to qualify this situation.

It is then not difficult to show that, using the $\{\mathbb{I}, \sigma_X, \sigma_Y, \sigma_Z\}$ Pauli matrices basis

$$\mathbb{I} = \begin{pmatrix} 1 & 0 \\ 0 & 1 \end{pmatrix}, \quad \sigma_X = \begin{pmatrix} 0 & 1 \\ 1 & 0 \end{pmatrix}, \quad \sigma_Y = \begin{pmatrix} 0 & -\mathrm{i} \\ \mathrm{i} & 0 \end{pmatrix}, \quad \sigma_Z = \begin{pmatrix} 1 & 0 \\ 0 & -1 \end{pmatrix}, \tag{19}$$

matrix B^2 defined in (4) approximatively reads

$$B^2 \simeq \omega_0^2 \mathbb{I} + \omega_0 \Omega_0 (\cos\phi_e \, \sigma_Z - \sin\phi_e \, \sigma_X), \tag{20a}$$

with

$$\Omega_0 = \sqrt{\Delta^2 + \kappa^2 \omega_0^2}, \quad \cos\phi_e = \frac{\Delta}{\Omega_0}, \quad \sin\phi_e = \frac{\kappa\omega_0}{\Omega_0}. \tag{20b}$$

Moreover, as explained in subsection 4.1 of [1], the starred terms in the right-hand side of equations (14) give no secular contribution to the time-evolutions of the Glauber variables α_1 and α_2, so that these equations are simplified§ into

$$\dot{\alpha}_1 = -\mathrm{i}\omega_1 \alpha_1 + \mathrm{i}\frac{\kappa\omega_0}{2}\alpha_2, \tag{21a}$$

$$\dot{\alpha}_2 = -\mathrm{i}\omega_2 \alpha_2 + \mathrm{i}\frac{\kappa\omega_0}{2}\alpha_1 \tag{21b}$$

(where ω_0 has been substituted for $\sqrt{\omega_1\omega_2}$, owing to the quasi-degeneracy situation). It is noteworthy that the above *approximate* equations (21) can be derived very simply from the *exact* equations (16) in the framework of quasi-degeneracy. Since $\omega_1 \simeq \omega_2 \simeq \omega_+ \simeq \omega_- \simeq \omega_0$ indeed, one can substitute ω_0 for $(\omega_1, \omega_2, \omega_+, \omega_-)$ in the definitions (12a) and (15a) themselves of the Glauber variables $(\alpha_1, \alpha_2, \alpha_+, \alpha_-)$. Then, using the (exact) relations (7) and (10), we get

$$q = P_e \varphi, \quad p = P_e \pi \quad \rightsquigarrow \begin{pmatrix} \alpha_1 \\ \alpha_2 \end{pmatrix} = P_e \begin{pmatrix} \alpha_+ \\ \alpha_- \end{pmatrix}. \tag{22}$$

Deriving (22) with respect to time, one has, owing to (16),

$$\begin{pmatrix} \dot{\alpha}_1 \\ \dot{\alpha}_2 \end{pmatrix} = -\mathrm{i} P_e \begin{pmatrix} \omega_+ & 0 \\ 0 & \omega_- \end{pmatrix} P_e^{-1} \begin{pmatrix} \alpha_1 \\ \alpha_2 \end{pmatrix}, \tag{23a}$$

which reads, allowing for (6), (20a), (20b) and $\Omega_0 \ll \omega_0$:

$$\begin{aligned} \begin{pmatrix} \dot{\alpha}_1 \\ \dot{\alpha}_2 \end{pmatrix} &= -\mathrm{i} \begin{pmatrix} \omega_0 + \frac{1}{2}\Omega_0 \cos\phi_e & -\frac{1}{2}\Omega_0 \sin\phi_e \\ -\frac{1}{2}\Omega_0 \sin\phi_e & \omega_0 - \frac{1}{2}\Omega_0 \cos\phi_e \end{pmatrix} \begin{pmatrix} \alpha_1 \\ \alpha_2 \end{pmatrix} \\ &= -\mathrm{i} \begin{pmatrix} \omega_1 & -\frac{1}{2}\kappa\omega_0 \\ -\frac{1}{2}\kappa\omega_0 & \omega_2 \end{pmatrix} \begin{pmatrix} \alpha_1 \\ \alpha_2 \end{pmatrix}, \end{aligned} \tag{23b}$$

so that equations (21) are recovered.

The above relation (22) deserves a further comment. Since matrix P_e is orthogonal, one has

$$|\alpha_1|^2 + |\alpha_2|^2 = |\alpha_+|^2 + |\alpha_-|^2 = N. \tag{24}$$

In other words, the *total* semiclassical quanta number N is an *intrinsic* quantity, in that it does not depend of the set of variables (standard or normal) which is used to calculate it. More generally, relation (22) suggests to consider (α_1, α_2) and (α_+, α_-) as the components of a "state" vector $|\psi\rangle$ in two different (orthonormalized) bases $\{|1\rangle, |2\rangle\}$ and $\{|+\rangle, |-\rangle\}$ of a two-dimensional Hilbert space $\hat{\mathcal{E}}$, and to write

$$|\psi(t)\rangle = \alpha_1(t)|1\rangle + \alpha_2(t)|2\rangle = \alpha_+(t)|+\rangle + \alpha_-(t)|-\rangle. \tag{25}$$

§ This simplification is known as the "Secular Approximation" (SA). It is introduced and used in [1] and [2].

With these notations, equations (21) as well as (16) read

$$\mathrm{i}\hbar\frac{\mathrm{d}|\psi(t)\rangle}{\mathrm{d}t} = \widehat{\mathcal{H}}|\psi(t)\rangle, \tag{26}$$

where $\widehat{\mathcal{H}}$ is a Hermitian operator respectively represented in bases $\{|1\rangle, |2\rangle\}$ and $\{|+\rangle, |-\rangle\}$ by the matrices:

$$\mathcal{H}_{1,2} = \begin{pmatrix} \hbar\omega_1 & -\kappa\frac{\hbar\omega_0}{2} \\ -\kappa\frac{\hbar\omega_0}{2} & \hbar\omega_2 \end{pmatrix} \text{ and } \mathcal{H}_{+,-} = \begin{pmatrix} \hbar\omega_+ & 0 \\ 0 & \hbar\omega_- \end{pmatrix}, \tag{27a}$$

with of course

$$\mathcal{H}_{+,-} = P_e^{-1}\mathcal{H}_{1,2}P_e. \tag{27b}$$

In the framework of this new description, it is noteworthy that vectors $|1\rangle$, $|2\rangle$, $|+\rangle$ and $|-\rangle$ have very simple meanings: vector $|1\rangle$ describes a state of the two-pendulum system in which pendulum 1 oscillates with an oscillation energy corresponding to one quantum $\hbar\omega_1$, pendulum 2 being at rest (more precisely : $\alpha_1 = 1$, $\alpha_2 = 0$); vector $|2\rangle$, conversely, describes the oscillation state ($\alpha_1 = 0$, $\alpha_2 = 1$). In the same way, vector $|+\rangle$ describes a state with one energy quantum $\hbar\omega_+$ in eigenmode $+$, eigenmode $-$ being "off" ($\alpha_+ = 1$, $\alpha_- = 0$); with of course the symmetric definition for vector $|-\rangle$ ($\alpha_+ = 0$, $\alpha_- = 1$). Let us recall that the above simplest definition of the physical states of the two-pendulum system entirely relies on the fulfilment of the quasi-degeneracy conditions.

2.2.2. Geometrical description of the movement : the Larmor space and the Bloch sphere As well known in QM, the time-evolution of the physical state of any two-level system in its two-dimensional (complex) Hilbert space can be represented by the motion of a (real) vector $\vec{m}$ in a $\mathbb{R}^3$-isomorphous space. Not surprisingly, this description can be applied to our (quasidegenerate) two-pendulum system.

To begin with, let us introduce the so-called "density-operator"

$$\hat{D}(t) = |\psi(t)\rangle\langle\psi(t)|. \tag{28}$$

In basis $\{|1\rangle, |2\rangle\}$, $\hat{D}$ is represented by the matrix

$$D = \begin{pmatrix} \alpha_1 \\ \alpha_2 \end{pmatrix} \begin{pmatrix} \alpha_1^* & \alpha_2^* \end{pmatrix} = \begin{pmatrix} \alpha_1\alpha_1^* & \alpha_1\alpha_2^* \\ \alpha_2\alpha_1^* & \alpha_2\alpha_2^* \end{pmatrix}. \tag{29a}$$

Expanding D in terms of the $\{\mathbb{I}, \sigma_X, \sigma_Y, \sigma_Z\}$ Pauli basis (see (19)), one gets

$$D = \frac{1}{2}\big(N\mathbb{I} + m_{X_0}\sigma_X + m_{Y_0}\sigma_Y + m_{Z_0}\sigma_Z\big) \tag{29b}$$

with

$$\begin{aligned} N &= \alpha_1\alpha_1^* + \alpha_2\alpha_2^*, \\ m_{X_0} &= \alpha_1^*\alpha_2 + \alpha_1\alpha_2^*, \\ m_{Y_0} &= -\mathrm{i}(\alpha_1^*\alpha_2 - \alpha_1\alpha_2^*), \\ m_{Z_0} &= \alpha_1\alpha_1^* - \alpha_2\alpha_2^*. \end{aligned} \tag{29c}$$

The above definitions are the classical adaptation of an algebra introduced by Schwinger [7], and ultimately reprinted in [8]. It is easy to check that

$$N^2 = m_{X_0}^2 + m_{Y_0}^2 + m_{Z_0}^2, \tag{30a}$$

and to establish (using Poisson's brackets (13))

$$\{m_{X_0}, m_{Y_0}\} = \frac{2m_{Z_0}}{\hbar}, \quad \{m_{Y_0}, m_{Z_0}\} = \frac{2m_{X_0}}{\hbar}, \quad \{m_{Z_0}, m_{X_0}\} = \frac{2m_{Y_0}}{\hbar}, \tag{30b}$$

as well as

$$\{N, m_{X_0}\} = \{N, m_{Y_0}\} = \{N, m_{Z_0}\} = 0. \tag{30c}$$

The above relations (30) (which, by the way, owe nothing to quasi-degeneracy), suggest that m_{X_0}, m_{Y_0} and m_{Z_0} are the three components of a *pseudo* dimensionless angular momentum $\vec{m}$ in some orthonormalized basis $\{\vec{e}_{X_0}, \vec{e}_{Y_0}, \vec{e}_{Z_0}\}$ of a *fictitious* $\mathbb{R}^3$ space, referred to as the "Larmor space" and henceforth labelled $\mathbb{L}$:

$$\vec{m} = m_{X_0}\vec{e}_{X_0} + m_{Y_0}\vec{e}_{Y_0} + m_{Z_0}\vec{e}_{Z_0}. \tag{30d}$$

Of course, the density operator $\hat{D}$ (see (28)) can be expanded all the same in the eigenstates basis $\{|+\rangle, |-\rangle\}$ of the Hilbert space $\hat{\mathcal{E}}$. It is then represented by the matrix

$$D_e = \begin{pmatrix} \alpha_+ \\ \alpha_- \end{pmatrix} \begin{pmatrix} \alpha_+^* & \alpha_-^* \end{pmatrix} = \begin{pmatrix} \alpha_+\alpha_+^* & \alpha_+\alpha_-^* \\ \alpha_-\alpha_+^* & \alpha_-\alpha_-^* \end{pmatrix}, \tag{31a}$$

which can in turn be expanded in terms of the Pauli basis (19):

$$D_e = \frac{1}{2}\big(N_e\mathbb{I} + m_X\sigma_X + m_Y\sigma_Y + m_Z\sigma_Z\big), \tag{31b}$$

with

$$\begin{array}{rcl} N_e &=& \alpha_+\alpha_+^* + \alpha_-\alpha_-^*, \\ m_X &=& \alpha_+^*\alpha_- + \alpha_+\alpha_-^*, \\ m_Y &=& -\,\mathrm{i}(\alpha_+^*\alpha_- - \alpha_+\alpha_-^*), \\ m_Z &=& \alpha_+\alpha_+^* - \alpha_-\alpha_-^*. \end{array} \tag{31c}$$

We still have $N_e^2 = m_X^2 + m_Y^2 + m_Z^2$ (see (30*a*)), as well as the commutation relations (30*b*). We can consequenltly all the same regard m_X, m_Y and m_Z as the components of a *pseudo* angular momentum $\vec{m}_e$ "living" in a $\mathbb{R}^3$-isomorphous space $\mathbb{L}_e$.

Nevertheless, it is *only* in the quasi-degeneracy limit that our representation reaches its full significance and interest. In this limit indeed, the Larmor spaces $\mathbb{L}_e$ and $\mathbb{L}$ *do coincide*, with

$$\vec{m}_e = \vec{m} = m_X\vec{e}_X + m_Y\vec{e}_Y + m_Z\vec{e}_Z, \tag{32a}$$

where the new orthonormalized basis $\{\vec{e}_X, \vec{e}_Y, \vec{e}_Z\}$ derives from $\{\vec{e}_{X_0}, \vec{e}_{Y_0}, \vec{e}_{Z_0}\}$ through the relations

$$\begin{array}{rcl} \vec{e}_X &=& \cos\phi_e\,\vec{e}_{X_0} + \sin\phi_e\,\vec{e}_{Z_0}, \\ \vec{e}_Y &=& \vec{e}_{Y_0}, \\ \vec{e}_Z &=& -\sin\phi_e\,\vec{e}_{X_0} + \cos\phi_e\,\vec{e}_{Z_0}, \end{array} \tag{32b}$$

i.e. through a rotation with angle $-\phi_e$ around common axis $\vec{e}_Y = \vec{e}_{Y_0}$ (see figure 2). Note by the way that equations (32) are the exact transposition in the Larmor space $\mathbb{L}$ of equations (22), (25) in the Hilbert space $\hat{\mathcal{E}}$. They imply *inter alia* $N_e = N$, as displayed by (24).

In order to describe the time-evolution of vector $\vec{m}$, one may solve equations (16) for (α_+, α_-) (resp. eqs. (21) for (α_1, α_2)), then use definitions (31*c*) of (m_X, m_Y, m_Z) (resp. (29*c*) of $(m_{X_0}, m_{Y_0}, m_{Z_0})$). In fact, there is a much smarter method. Let us consider again equations (21). They obviously derive from the secular‖ Hamiltonian

$$H^{\mathrm{sec}} = \hbar\omega_1|\alpha_1|^2 + \hbar\omega_2|\alpha_2|^2 - \kappa\frac{\hbar\omega_0}{2}(\alpha_1\alpha_2^* + \alpha_1^*\alpha_2). \tag{33a}$$

‖ This term is explained in [1]. It originates from the fact that the *numerical* value of H^{sec} varies *slowly* at the time-scale of ω_0^{-1}.

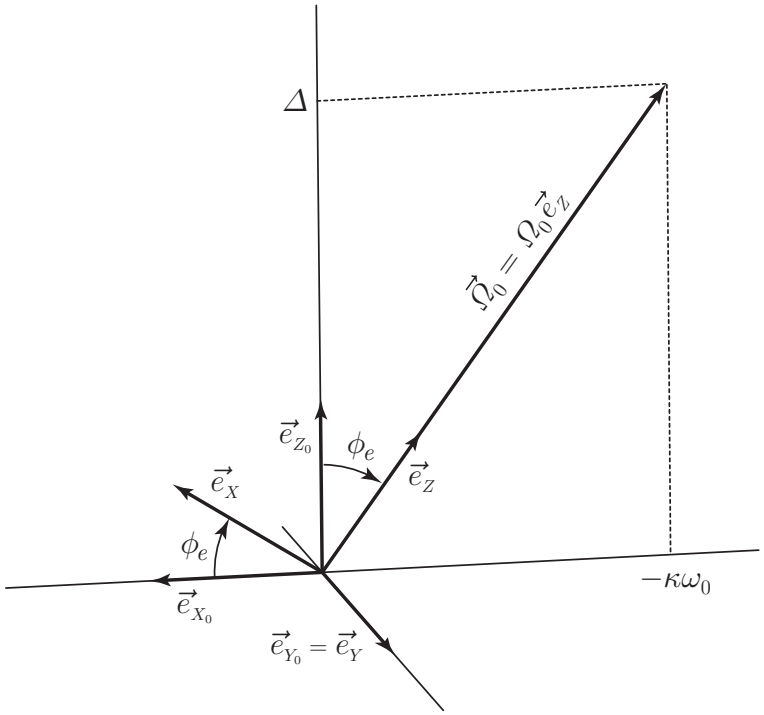

Figure 2. Main elements of the geometrical representation of the free motion of (any) quasidegenerate HO2 in its Larmor space. The representing vector $\vec{m}$ precesses with the angular velocity $\vec{\Omega}_0 = \Delta\,\vec{e}_{Z_0} - \kappa\omega_0\,\vec{e}_{X_0} = \Omega_0\,\vec{e}_Z$. Basis $\{\vec{e}_X, \vec{e}_Y, \vec{e}_Z\}$ is derived from $\{\vec{e}_{X_0}, \vec{e}_{Y_0}, \vec{e}_{Z_0}\}$ through a rotation with angle $-\phi_e$ around common axis $\vec{e}_Y = \vec{e}_{Y_0}$.

Using definition (29c), the above Hamiltonian can be rewritten

$$H^{\rm sec} = N\hbar\omega_0 + \frac{\hbar}{2}\vec{\Omega}_0 \cdot \vec{m}, \tag{33b}$$

where

$$\vec{\Omega}_0 = \Delta\,\vec{e}_{Z_0} - \kappa\omega_0\,\vec{e}_{X_0} \tag{33c}$$

is the so-called Larmor precession angular velocity. Using Poisson's brackets (30b), (30c), the Ehrenfest theorem reads indeed

$$\frac{{\rm d}\vec{m}}{{\rm d}t} = \{\vec{m}, H^{\rm sec}\} = \vec{\Omega}_0 \times \vec{m}\,; \qquad \frac{{\rm d}N}{{\rm d}t} = \{N, H^{\rm sec}\} = 0. \tag{34}$$

The time-evolution of $\vec{m}$ is thus a precession with angular velocity $\vec{\Omega}_0$. The main features of the geometrical representation of the free motion of the quasidegenerate two-pendulum system (in fact of *any* quasidegenerate HO2) are displayed in figure 2.

To complete this brief overflight of our adapting the Schwinger representation to the two-pendulum problem, it is interesting to recall how the basis vectors $|1\rangle$, $|2\rangle$, $|+\rangle$ and $|-\rangle$ introduced above about the Hilbert space $\hat{\mathcal{E}}$ are represented in the Larmor space $\mathbb{L}$. Unit vector $|1\rangle$ in $\hat{\mathcal{E}}$ is represented by unit vector $\vec{e}_{Z_0}$ in $\mathbb{L}$. Conversely, vector $|2\rangle$ in $\hat{\mathcal{E}}$ is represented by unit vector $-\vec{e}_{Z_0}$ in $\mathbb{L}$. Similarly, unit vectors $|+\rangle$ and $|-\rangle$

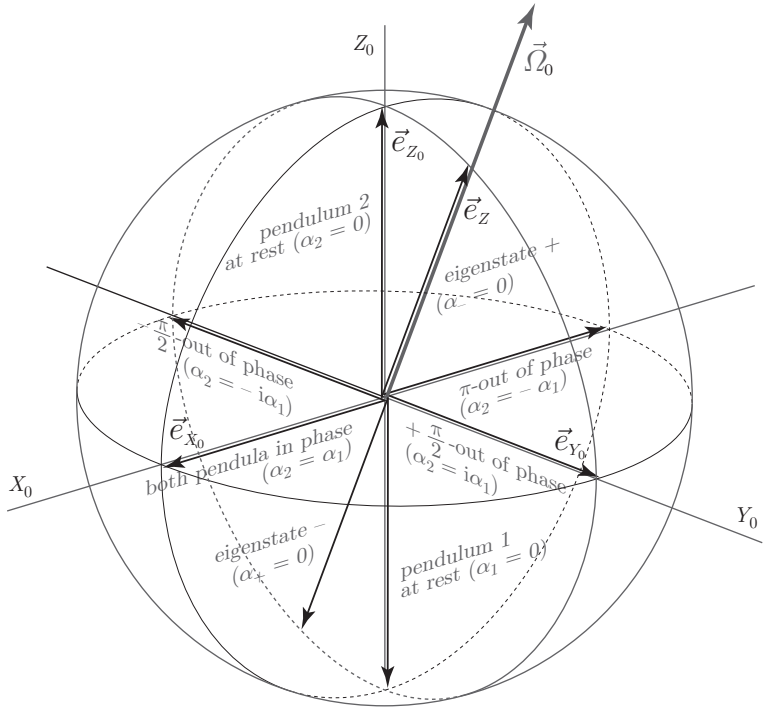

Figure 3. A few remarkable orientations of the representing vector $\vec{m}$ in the Larmor space. We have displayed the Bloch sphere with radius $N = 1$. Along axis X_0, the pendula are in phase ($\vec{e}_{X_0}$) or π-out of phase ($-\vec{e}_{X_0}$). Along axis Y_0, the pendula are $\pm\frac{\pi}{2}$-out of phase ($\pm\vec{e}_{Y_0}$). Along axis Z_0, pendulum 2 or pendulum 1 is at rest ($\vec{e}_{Z_0}$ or $-\vec{e}_{Z_0}$ respectively). Along the $\vec{\Omega}_0$ direction, the two-pendulum system is in its eigenstates + or − ($\vec{e}_Z$ or $-\vec{e}_Z$ respectively).

in $\hat{\mathcal{E}}$ are represented by unit vectors $\vec{e}_Z$ and $-\vec{e}_Z$, respectively. It is noteworthy that vectors $|1\rangle$ and $|2\rangle$ on the one hand, vectors $|+\rangle$ and $|-\rangle$ on the other hand, are orthogonal in $\hat{\mathcal{E}}$, while they are represented by opposite vectors in $\mathbb{L}$. This rule is general: if $|\psi_1\rangle$ and $|\psi_2\rangle$ are orthogonal in space $\hat{\mathcal{E}}$, then their representations $\vec{m}_1$ and $\vec{m}_2$ make an angle equal to π in space $\mathbb{L}$. As displayed by (29c), *any* vector of $\hat{\mathcal{E}}$ has a representation in $\mathbb{L}$. Reciprocally, we have shown in [1] that every vector of $\mathbb{L}$ is the representation of a state vector of $\hat{\mathcal{E}}$. Nevertheless, this $\hat{\mathcal{E}} \leftrightarrow \mathbb{L}$ correspondance is not strictly speaking biunivocal: vectors $|\psi\rangle$ and $e^{i\chi}|\psi\rangle$ (χ real) of $\hat{\mathcal{E}}$ are represented by the *same* vector $\vec{m}$ of $\mathbb{L}$. This is due to the fact that the phase factor $e^{i\chi}$ is lost when one builds the density operator $\hat{D}$ (see definition (28)). Moreover, any unit vector of $\hat{\mathcal{E}}$ is represented by a unit vector of $\mathbb{L}$. Thus, the tips of all vectors $\vec{m}$ describing physical states with a *given* total (semiclassical) quanta number, say N, are located in $\mathbb{L}$ on the surface of a sphere with centre at the origin and radius N. Such a sphere will be referred to as a "Bloch sphere" throughout the present paper. The Bloch sphere with radius unity is displayed in figure 3, as well as a few remarkable orientations of vector $\vec{m}$ mentioned above.

As displayed by equations (34), in any *free* movement of the quasidegenerate

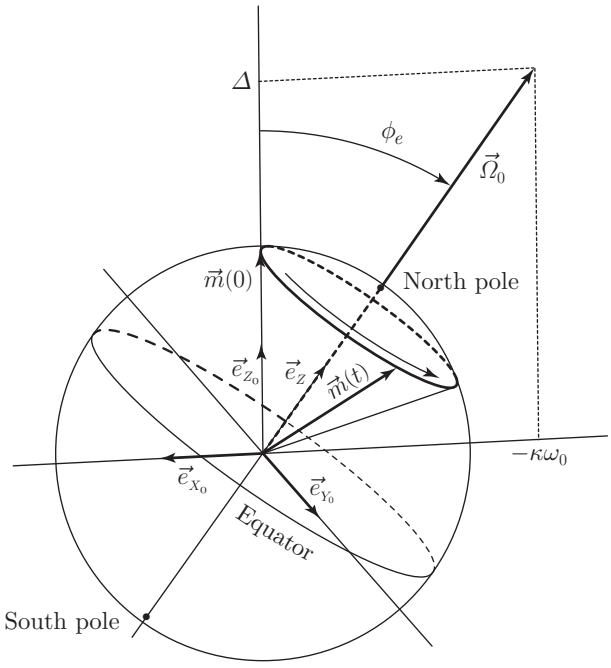

Figure 4. Representation of the free movement in the Larmor space in the particular case where $\vec{m}(0) = N\vec{e}_{Z_0}$ (*i.e.* only pendulum 1 excited, with N oscillation quanta). The pseudo angular momentum $\vec{m}$ undergoes a rotation around axis $\vec{e}_Z$ with constant angular velocity Ω_0 (Larmor precession). The representative point (*i.e.* $\vec{m}$'s tip) moves on a parallel of its Bloch sphere and thus keeps at a constant distance from both poles.

HO2, the total semiclassical quanta number N is conserved¶, which means that the tip of vector $\vec{m}$ (in $\mathbb{L}$) moves on the surface of a Bloch sphere. This is the geometrical translation of the unitarity of the time-evolution of vector $|\psi(t)\rangle$ (in $\hat{\mathcal{E}}$), as involved by the Schrödinger-like equation (26). Moreover, allowing for (34) again, the angle between $\vec{\Omega}_0$ and $\vec{m}$ is constant too: $\vec{m}(t)$ generates a cone, the apex half-angle of which is fixed by the initial conditions. This cone is displayed in figure 4 (in the particular case where $\vec{m}(0) = N\vec{e}_{Z_0}$, *i.e.* where only pendulum 1 is oscillating at $t = 0$, with N oscillation quanta). The trajectory of the representative point (*i.e.* the tip of vector $\vec{m}(t)$ on its Bloch sphere) is a circle with axis $\vec{\Omega}_0$. From now on and by convention, we shall call "North pole" (resp. "South pole") the intersection of the Bloch sphere with the semi-axis $+Z$ (resp. $-Z$). With this "geographical" vocabulary, it is clear that in any *free* motion of the two-pendulum system, the representative point moves on a parallel of the Bloch sphere, and thus keeps at a constant distance from both poles.

Could we manage to obtain a more complex trajectory of the representative point on the Bloch sphere, for instance a trip from one pole to the other? We shall show below that the answer is yes.

¶ Using the time-honoured jargon of QM, N is said to be a "good quantum number".

3. Parametric excitation of the two-pendulum system

There are several ways to implement a parametric excitation of the two-pendulum system. One may vary the apparent gravity by fixing axis (A) (see figure 1) in a (vertically) accelerated frame. One may also vary the stiffness C of the coupling device. At last, one may vary the length (ℓ_1, ℓ_2 or both) of the pendula. In the above schemes, the dynamical matrix B^2 (see (4)) and the orthogonal passage matrix P_e (see (6b)) become time-dependent, as well as the definition (12a) of the Glauber variables, so that the motion equations (14) are non longer valid. Let us examine this point.

3.1. The general case

It is easy to check that Lagrangian

$$L(\theta_1,\theta_2,\dot\theta_1,\dot\theta_1,t)=\frac{1}{2}J_1\dot\theta_1^2+\frac{1}{2}J_2\dot\theta_2^2-\frac{1}{2}Mg\ell_1\theta_1^2-\frac{1}{2}Mg\ell_2\theta_2^2-\frac{1}{2}C(\theta_1-\theta_2)^2 \qquad (35a)$$

is available to describe the dynamics of the system, even if parameters ℓ_1 ($\rightsquigarrow J_1$), ℓ_2 ($\rightsquigarrow J_2$), g or C are varied in the course of the (small) oscillations of the pendula. Consequently, Hamiltonian

$$H(\theta_1,\theta_2,\sigma_1,\sigma_2,t)=\frac{\sigma_1^2}{2J_1}+\frac{\sigma_2^2}{2J_2}+\frac{1}{2}Mg\ell_1\theta_1^2+\frac{1}{2}Mg\ell_2\theta_2^2+\frac{1}{2}C(\theta_1-\theta_2)^2, \qquad (35b)$$

where

$$\sigma_k=\frac{\partial L}{\partial\dot\theta_k}\quad(k=1,2), \qquad (35c)$$

is available too. Then, using definitions (2b) and (2c) (which are now time-dependent), and rewriting definition (12a) as

$$\alpha_k=\frac{1}{\sqrt{2\hbar}}\left(\sqrt{\omega_kJ_k}\theta_k+\frac{\mathrm{i}}{\sqrt{\omega_kJ_k}}\sigma_k\right), \qquad (35d)$$

it turns out that expression (12b) of the Hamiltonian is still valid, even with ω_1, ω_2 or κ being time-dependent. Nevertheless the motion equations (14) should now be completed using the generalized Ehrenfest relations

$$\dot\alpha_1=\{\alpha_1,H\}+\frac{\partial\alpha_1}{\partial t}=-\mathrm{i}\omega_1(t)\alpha_1+\frac{\mathrm{i}}{2}(\kappa\sqrt{\omega_1\omega_2})(t)(\alpha_2+\alpha_2^*)+f_1(t)\alpha_1^*, \qquad (36a)$$

$$\dot\alpha_2=\{\alpha_2,H\}+\frac{\partial\alpha_2}{\partial t}=-\mathrm{i}\omega_2(t)\alpha_2+\frac{\mathrm{i}}{2}(\kappa\sqrt{\omega_1\omega_2})(t)(\alpha_1+\alpha_1^*)+f_2(t)\alpha_2^*, \qquad (36b)$$

with

$$f_k(t)=\frac{1}{2}\frac{\dot{\left(J_k\omega_k\right)}}{J_k\omega_k}=\frac{\mathrm{d}}{\mathrm{d}t}\ln\sqrt{J_k\omega_k}\quad(k=1,2). \qquad (36c)$$

The above equations are exact. Nevertheless, trying to solve them for (α_1,α_2) leads to cumbersome calculations, and no analytical solution is available. In a foregoing study [9] we have tackled this question in the general framework of the n-degree-of-freedom parametrically excited harmonic oscillator. Let us sketch below the main conclusions of this study.

The first idea that springs to mind is of course to introduce the *instantaneous* eigenmodes of the two-pendulum device and rewrite system (36) using the associated Glauber variables $\alpha_\pm(t)$. A (tedious) time-derivation of these variables leads to

$$\frac{\mathrm{d}}{\mathrm{d}t}\begin{pmatrix}\alpha_+\\ \alpha_-\end{pmatrix}=-\mathrm{i}\begin{pmatrix}\omega_+(t) & 0\\ 0 & \omega_-(t)\end{pmatrix}\begin{pmatrix}\alpha_+\\ \alpha_-\end{pmatrix}+\mathcal{A}\begin{pmatrix}\alpha_+\\ \alpha_-\end{pmatrix}+\mathcal{S}\begin{pmatrix}\alpha_+^*\\ \alpha_-^*\end{pmatrix}, \qquad (37)$$

where $\mathcal{S}$ is a symmetrical 2×2 matrix and $\mathcal{A}$ an antisymmetrical one. It is next shown that, if the parametric excitation is *adiabatic in the Ehrenfest sense* (see [9] for a detailed explanation of this term), then the total semiclassical *eigen* quanta number $N_e = |\alpha_+(t)|^2 + |\alpha_-(t)|^2$ is conserved in the course of the motion (whereas, separately, $|\alpha_+(t)|^2$ and $|\alpha_-(t)|^2$ are not), and is therefore an adiabatic invariant of the oscillator.

3.2. The quasi-degeneracy limit

3.2.1. Parametric excitation in the Hilbert space In the present paper, we shall not attempt to determine explicitly matrices $\mathcal{A}$ and $\mathcal{S}$ in the general case, but rather focus on the quasi-degeneracy limit. In the framework of this limit (and of the associated approximations) indeed, system (36) is simplified into

$$\dot{\alpha}_1 = -\mathrm{i}\omega_1(t)\alpha_1 + \frac{\mathrm{i}}{2}(\kappa\omega_0)(t)\alpha_2 + f_1(t)\alpha_1^*, \tag{38a}$$

$$\dot{\alpha}_2 = -\mathrm{i}\omega_2(t)\alpha_2 + \frac{\mathrm{i}}{2}(\kappa\omega_0)(t)\alpha_1 + f_2(t)\alpha_2^*. \tag{38b}$$

Furthermore, if the parametric excitation is adiabatic,[+] then the starred terms in the right-hand side of the above equations (38) can be omitted (they bring no secular contribution to the time-evolution of α_1 or α_2). We are thus left again with system (23b), in which ω_1, ω_2 and $\kappa\omega_0$ are now time-dependent.

On the other hand, as made in [9] in the general case, we can rewrite (38) using the eigen Glauber variables $\alpha_\pm$ in the framework of quasi-degeneracy. Allowing for (6b) and (22), we then recover (37), with matrices $\mathcal{A}$ and $\mathcal{S}$ now (approximately) given by

$$\mathcal{A} = -P_e^{-1}\dot{P}_e = \frac{\dot{\phi}_e}{2}\begin{pmatrix} 0 & -1 \\ 1 & 0 \end{pmatrix}, \tag{39a}$$

$$\mathcal{S} = P_e^{-1}\begin{pmatrix} f_1 & 0 \\ 0 & f_2 \end{pmatrix}P_e = \frac{1}{2}(f_1+f_2)\mathbb{I} + \frac{1}{2}(f_1-f_2)\begin{pmatrix} \cos\phi_e & \sin\phi_e \\ \sin\phi_e & -\cos\phi_e \end{pmatrix}. \tag{39b}$$

As recalled above about (37) and (38), the contribution of the starred terms in the right-hand sides is negligible in the case of an adiabatic excitation. In the latter case, building the state vector $|\psi(t)\rangle$ defined in (25), we recover the Schrödinger equation (26), with Hamiltonian $\hat{\mathcal{H}}$ now time-dependent and respectively represented in bases $\{|1\rangle, |2\rangle\}$ and $\{|+\rangle, |-\rangle\}$ by the matrices:

$$\mathcal{H}_{1,2}(t) = \begin{pmatrix} \hbar\omega_1(t) & -\frac{\hbar}{2}\kappa\omega_0(t) \\ -\frac{\hbar}{2}\kappa\omega_0(t) & \hbar\omega_2(t) \end{pmatrix} \quad \text{and} \quad \mathcal{H}_{+,-}(t) = \begin{pmatrix} \hbar\omega_+(t) & 0 \\ 0 & \hbar\omega_-(t) \end{pmatrix}. \tag{40}$$

We would emphasize the following point. Passing from the vectorial equation (26) to system (23b) is straightforward, since basis $\{|1\rangle, |2\rangle\}$ *does not* depend on time. *A contrario*, handling the Schrödinger equation in basis $\{|+\rangle, |-\rangle\}$ requires some care. Allowing for (6b) indeed, we have

$$\begin{aligned} \frac{\mathrm{d}|+\rangle}{\mathrm{d}t} &= -\frac{\dot{\phi}_e}{2}\Big(\sin\frac{\phi_e}{2}|1\rangle + \cos\frac{\phi_e}{2}|2\rangle\Big) = -\frac{\dot{\phi}_e}{2}|-\rangle, \\ \frac{\mathrm{d}|-\rangle}{\mathrm{d}t} &= \frac{\dot{\phi}_e}{2}\Big(\cos\frac{\phi_e}{2}|1\rangle - \sin\frac{\phi_e}{2}|2\rangle\Big) = \frac{\dot{\phi}_e}{2}|+\rangle, \end{aligned} \tag{41a}$$

[+] Under the circumstances, "adiabatic" means "slow at the time-scale of the free motion": rates f_1 and f_2 (see (36c)), as well as all the angular frequencies of their nonzero Fourier components, are *small* compared to ω_0.

so that expanding (26) on basis $\{|+\rangle, |-\rangle\}$ yields, non surprisingly (see (39a)),

$$\begin{pmatrix} \dot{\alpha}_+ \\ \dot{\alpha}_- \end{pmatrix} = \begin{pmatrix} -\mathrm{i}\omega_+ & -\frac{\dot{\phi}_e}{2} \\ \frac{\dot{\phi}_e}{2} & -\mathrm{i}\omega_- \end{pmatrix} \begin{pmatrix} \alpha_+ \\ \alpha_- \end{pmatrix}. \tag{41b}$$

The off-diagonal terms of the above matrix are responsible for *transitions* between the two eigenstates of Hamiltonian operators $\hat{\mathcal{H}}(t)$. These off-diagonal terms originate in the time-dependence of basis vectors $|+\rangle$ and $|-\rangle$, as displayed by relations (41a). This result is remarkable: should the (adiabatic) parametric excitation of the two-pendulum system not "mix" its eigenmodes, then both $N_+ = |\alpha_+|^2$ and $N_- = |\alpha_-|^2$ would *separately* be conserved in the course of the motion (in other words, the HO2 would behave as the simple juxtaposition of two noninteracting HO2).

3.2.2. Parametric excitation in the Larmor space Correlatively, in the Larmor space $\mathbb{L}$, the movement of the pseudo angular momentum $\vec{m}$ is still governed by equation (24) in which $\vec{\Omega}_0(t)$ now depends on time, not only in intensity but also in *direction*. In the latter dependence originate $\vec{m}$-flips between $+\vec{e}_Z$ and $-\vec{e}_Z$, which are the exact representation of the above-mentioned $|\psi\rangle$-transitions between $|+\rangle$ and $|-\rangle$, and which can be simply apprehended as follows. Let us consider again the orthonormalized basis $\{\vec{e}_X, \vec{e}_Y, \vec{e}_Z\}$ defined in (32b). This basis is now time-dependent and we have

$$\dot{\vec{e}}_X = \dot{\phi}_e\, \vec{e}_Z, \quad \dot{\vec{e}}_Y = 0, \quad \dot{\vec{e}}_Z = -\dot{\phi}_e\, \vec{e}_X, \tag{42a}$$

so that equation (34) yields

$$\begin{aligned} \dot{m}_X &= -\Omega_0(t)\, m_Y + \dot{\phi}_e\, m_Z, \\ \dot{m}_Y &= +\Omega_0(t)\, m_X, \\ \dot{m}_Z &= -\dot{\phi}_e\, m_X. \end{aligned} \tag{42b}$$

Observe that the above results (42) are the exact trasposition to the Larmor space $\mathbb{L}$ of the foregoing equations (41) in the Hilbert space $\hat{\mathcal{E}}$. Note too that, since $\dot{\phi}_e \neq 0$, component m_Z is no longer constant as was the case in the free Larmor precession with static angular frequency $\vec{\Omega}_0$.

We shall now focus on a particular case of adiabatic parametric excitation of our HO2 inducing the classical equivalent of the "Rabi precession". In this case, the machinery of the aforesaid transitions/flips can be clearly demonstrated and calculated, as well in the Hilbert space as in the Larmor one.

4. Simulating the Rabi precession

4.1. The experimental device

Let us come back to the experimental device displayed in figure 1, and let us modify it in the following way. In one of the pendula, say number 1, the cylinder can be slid along the rods thanks to a piano wire drawn (up or down) by an electric engine. We should precise that, in the latter movement, the wire is dragged through a grooved pulley located on axis (A), so that no torque at all is exerted onto this axis by the wire's doing: moving the mass along the rod simply changes its distance to axis (A) and should thus be regarded as a pure parametric excitation of the pendulum. This modified device is displayed in figure 5. Let the electric engine rotate at angular

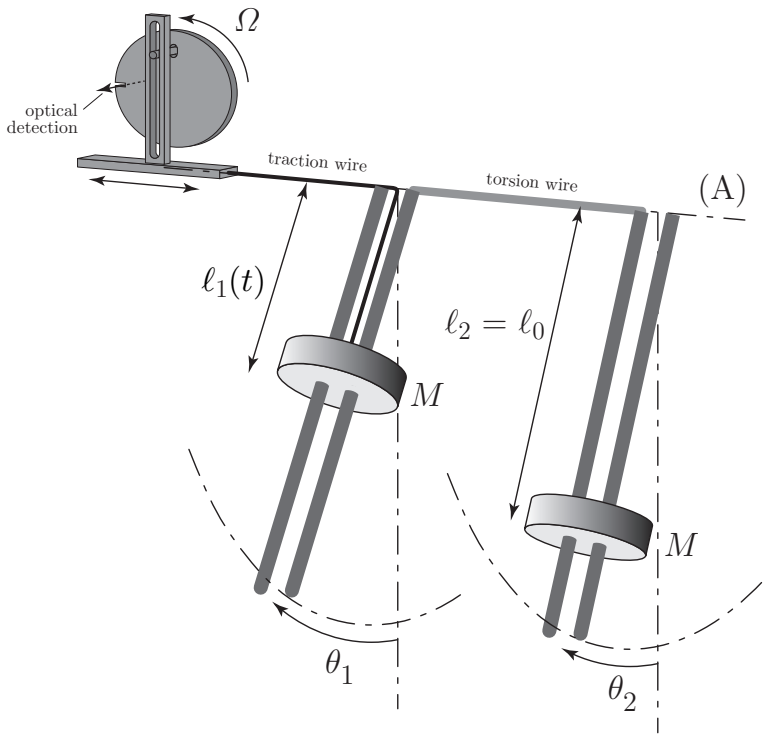

Figure 5. Modified experimental device. In the left pendulum, labelled 1, the cylindrical mass M can be slid along a couple of rods thanks to a traction wire dragged by an electric engine through a grooved pulley in such a way that no torque at all is exerted upon (A): sliding mass M thus implements a pure parametric excitation of pendulum 1.

frequency $\Omega \ll \omega_0$. This results in a modulation of distance ℓ_1 which reads (omitting index 0 for the mean value):

$$\ell_1 + \delta\ell_1(t) = \ell_1(1 + \epsilon \sin \Omega t). \tag{43a}$$

We shall henceforth assume that the above modulation is *small*: $\epsilon \ll 1$. We then get, after simple calculations,

$$\omega_1 + \delta\omega_1(t) = \omega_1 \left(1 + \frac{1}{2}\left(\frac{Mg\ell_1}{Mg\ell_1 + C} - \frac{J_1'\ell_1}{J_1}\right)\epsilon \sin \Omega t\right), \tag{43b}$$

$$\kappa\omega_0 + \delta(\kappa\omega_0)(t) = \kappa\omega_0 \left(1 - \frac{1}{4}\left(\frac{Mg\ell_1}{Mg\ell_1 + C} + \frac{J_1'\ell_1}{J_1}\right)\epsilon \sin \Omega t\right), \tag{43c}$$

where $J_1' = \frac{\mathrm{d}J_1}{\mathrm{d}\ell_1}$. One has in addition, as a consequence of (17):

$$\delta\omega_0(t) = \frac{1}{2}\delta\omega_1(t), \qquad \delta\Delta(t) = \delta\omega_1(t). \tag{44}$$

Observe that the above expressions (43*b*, c) can be drastically simplified, at least in first approximation: the coupling is *small*, then (see (2*c*)) $C \ll Mg\ell_1$; the pendula are quasi *simple* ones, thus $J_1 \simeq M\ell_1^2 \rightsquigarrow \frac{J_1'\ell_1}{J_1} \simeq 2$; in addition $\omega_1 \simeq \omega_0$ (quasi-degeneracy).

As a consequence of the above approximations, we have *roughly*:

$$\delta\Delta(t) = \delta\omega_1(t) \simeq -\frac{1}{2}\omega_0\epsilon\sin\Omega t, \tag{45a}$$

$$\delta(\kappa\omega_0) \simeq -\frac{3}{4}\kappa\omega_0\epsilon\sin\Omega t. \tag{45b}$$

The above relations (45) show that, since $\kappa \ll 1$, the modulation of $\kappa\omega_0$ is small compared to that of Δ, and can therefore be neglected. Consequently

$$\delta\vec{\Omega}_0(t) \simeq \delta\Delta(t)\vec{e}_{Z_0}, \quad \delta\Omega_0(t) \simeq \delta\Delta(t)\cos\phi_e, \quad \delta\phi_e(t) \simeq -\delta\Delta(t)\frac{\sin\phi_e}{\Omega_0}. \tag{46}$$

We shall now consider the physical consequences of the above-described (equations (43a) through (46)) slight modulation of length ℓ_1. For the sake of completeness and to underline the high suggestion power of the Larmor representation, we shall successively carry out the calculations in the Hilbert space $\hat{\mathcal{E}}$, then in the Larmor space $\mathbb{L}$. In the meantime, we shall illustrate our purpose with the results of our experimental implementation.

To begin with, let us consider the situation in the Hilbert space.

4.2. Calculation in the Hilbert space

Setting:

$$\begin{aligned} \alpha_+(t) &= C_+(t)\,\mathrm{e}^{-\mathrm{i}(\omega_0+\frac{\Omega}{2})t}, \\ \alpha_-(t) &= C_-(t)\,\mathrm{e}^{-\mathrm{i}(\omega_0-\frac{\Omega}{2})t}, \end{aligned} \tag{47}$$

and using secularized equations (41b), we obtain the system:

$$\mathrm{i}\begin{pmatrix} \dot{C}_+ \\ \dot{C}_- \end{pmatrix} = \begin{pmatrix} a & -\mathrm{i}b \\ \mathrm{i}b & a \end{pmatrix}\begin{pmatrix} C_+ \\ C_- \end{pmatrix}, \tag{48}$$

where

$$\begin{aligned} a(t) &= \frac{\Omega_0-\Omega}{2} - \frac{1}{4}\omega_0\varepsilon\cos\phi_e\,\sin\Omega t, \\ b(t) &= \frac{1}{4}\omega_0\varepsilon\sin\phi_e\,\frac{\Omega}{\Omega_0}\cos\Omega t\,\mathrm{e}^{-\mathrm{i}\Omega t}. \end{aligned} \tag{49}$$

From now on, to be consistent at first order in ϵ, the time-dependence of angle ϕ_e will be neglected in the above system (49). Moreover, (48) can be further simplified, provided that conditions (quite analogous with (18))

$$|\Omega_0-\Omega|, \;\; \Omega_{\mathrm{R}} = \frac{1}{4}\omega_0\varepsilon\sin\phi_e \ll \Omega_0 \tag{50a}$$

(Ω_{R} is the so-called "Rabi angular frequency") are *simultaneously* fulfilled, or equivalently that:

$$\Omega_{\mathrm{eff}} = \sqrt{(\Omega_0-\Omega)^2+\Omega_{\mathrm{R}}^2} \ll \Omega_0. \tag{50b}$$

In return indeed for the above conditions (50) fulfillement, system (48) is simplified into:

$$\mathrm{i}\begin{pmatrix} \dot{C}_+ \\ \dot{C}_- \end{pmatrix} = \frac{1}{2}\left[(\Omega_0-\Omega)\sigma_Z + \Omega_R\sigma_Y\right]\begin{pmatrix} C_+ \\ C_- \end{pmatrix}. \tag{51}$$

Then setting, in analogy with (20b):

$$\cos\beta = \frac{\Omega_0-\Omega}{\Omega_{\mathrm{eff}}}, \qquad \sin\beta = \frac{\Omega_{\mathrm{R}}}{\Omega_{\mathrm{eff}}}, \tag{52}$$

the above Schrödinger-like equation (51) is satisfied by the unitary evolution law:

$$\begin{pmatrix} C_+(t) \\ C_-(t) \end{pmatrix} = \begin{pmatrix} \cos\frac{\Omega_{\rm eff}t}{2} - {\rm i}\cos\beta\ \sin\frac{\Omega_{\rm eff}t}{2} & -\sin\beta\ \sin\frac{\Omega_{\rm eff}t}{2} \\ \sin\beta\ \sin\frac{\Omega_{\rm eff}t}{2} & \cos\frac{\Omega_{\rm eff}t}{2} + {\rm i}\cos\beta\ \sin\frac{\Omega_{\rm eff}t}{2} \end{pmatrix} \begin{pmatrix} C_+(0) \\ C_-(0) \end{pmatrix}. \quad (53)$$

Let us suppose, for instance, that the two-pendulum system is initially prepared in eigenmode (+), with N quanta, say: $\alpha_-(0) = 0$, $\alpha_+(0) = C_+(0) = \sqrt{N}$. Then we have:

$$\begin{aligned} |\alpha_+(t)|^2 &= |C_+(t)|^2 = N(1 - \sin^2\beta \sin^2\frac{\Omega_{\rm eff}t}{2}), \\ |\alpha_-(t)|^2 &= |C_-(t)|^2 = N\sin^2\beta \sin^2\frac{\Omega_{\rm eff}t}{2}, \end{aligned} \quad (54)$$

which is, by the way, the perfect transposition of formulas (68) in [1].

Thus the system undergoes transitions between modes (+) and (−). These transitions are complete only for $\beta = \frac{\pi}{2}$ ($\Omega_0 = \Omega$), *i.e.* at *resonance*. This parametrically induced movement is known as the "Rabi precession". Let us observe that, at resonance, the effective angular frequency $\Omega_{\rm eff}$ is minimum (and equal to $\Omega_{\rm R}$) and that, after an *odd* number of full Rabi precessions (*i.e.* at instants $t'_n = (2n+1)\frac{2\pi}{\Omega_{\rm eff}}$, with n integer), the state vector $|\psi\rangle$ of the system is left 180° out of phase with that of a twin device undergoing no parametrical excitation at all. An analogous remark has already been made about the induction-free movement (see (70) and the related comments in [1]). Moreover, let us keep in mind that the classical analogy of the Rabi precession we propose in the present paper relies on a twofold secular approximation: the SA was *already* used to simplify (37) into (48), which required the adiabatic condition $\Omega \ll \omega_0$. Further simplifying (48) into (51), which requires $\Omega_{\rm eff} \ll \Omega_0$, should consequently be regarded as a *second* secularization of (37). As a consequence and in prospect of an experimental check of results (53 - 54), we should, whatever the circumstances, maintain the twofold conditions fulfilled:

$$\Omega_{\rm R} \ll \Omega_0 \ll \omega_0, \quad (55a)$$

or equivalently (see (20*b*) and (50*a*)):

$$\epsilon \ll \kappa \ll 1. \quad (55b)$$

Let us now relate our experimental implementation of the Rabi precession.

4.3. Experimental results

As displayed by (41*b*) or (42*b*), the most effective manner to induce transitions between modes (+) and (−) of the HO2 is to maximize derivative $\dot{\phi}_e$, which corresponds, in the Larmor space, to $\delta\vec{\Omega}_0(t)$ perpendicular to $\vec{\Omega}_0$. Since, with our length modulation (43*a*), $\delta\vec{\Omega}_0(t)$ is parallel to $\vec{e}_{Z_0}$ (see (46)), we should set $\vec{\Omega}_0$ parallel to $\vec{e}_{X_0}$, *i.e.* have $\phi_e = \frac{\pi}{2}$. Consequently, the mean value ℓ_1 of $\ell_1(t)$ is fixed equal to ℓ_2, both pendula being thus identical in absence of parametric excitation. Allowing for (7) and (6*b*), the normal variables are then given by:

$$\varphi = \begin{pmatrix} \varphi_+ \\ \varphi_- \end{pmatrix} = {}^tP_e q = \sqrt{\frac{J}{2}} \begin{pmatrix} \theta_1 - \theta_2 \\ \theta_1 + \theta_2 \end{pmatrix}. \quad (56)$$

According to the above equation (56), mode (−) corresponds to both pendula in phase ($\theta_1 = \theta_2$) and mode (+) to both pendula 180°-out of phase with each other ($\theta_1 = -\theta_2$).

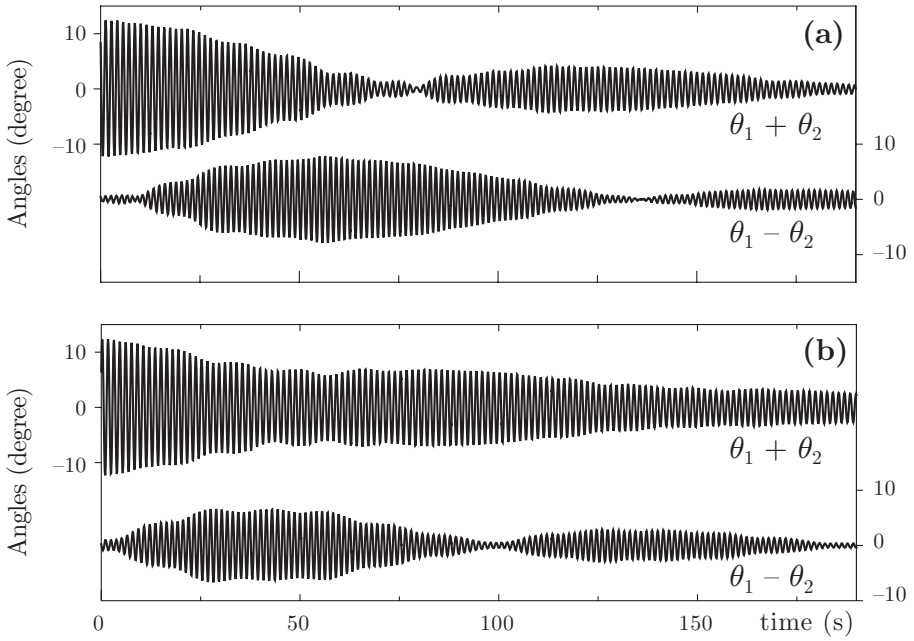

Figure 6. Examples of Rabi precessions: normal variables φ_+ and φ_- (respectively represented by $\theta_1 - \theta_2$ and $\theta_1 + \theta_2$) associated with modes (+) and (−), as functions of time. Both pendulum lengths are 53 cm and $\Omega_0 = 0.231 \pm 0.003$ rad/s. Initially, only mode (−) is excited. In (a), the angular frequency of the engine is $\Omega = 0.228 \pm 0.003$ rad/s $\simeq \Omega_0$: $\cos\beta \simeq 0$ and the transfer from mode (−) to mode (+) is total. In (b), $\Omega = 0.190 \pm 0.003$ rad/s $\neq \Omega_0$: $\cos\beta = 0.67$ and the transfer is but partial.

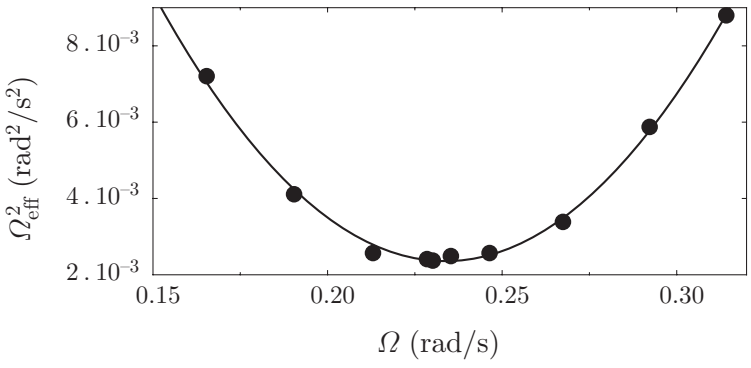

Figure 7. Square of the effective angular frequency $\Omega_{\rm eff}$ of the Rabi precession as a function of the angular frequency Ω of the engine. The expected law is given by (50*b*) with $\Omega_0 = 0.231$ rad/s and $\Omega_R = 4.85 \times 10^{-2}$ rad/s. The fit (solid curve) gives $\Omega_0 = 0.234$ rad/s and $\Omega_R = 4.85 \times 10^{-2}$ rad/s.

In figures 6, we have dispayed the quantities $\theta_1 + \theta_2$ and $\theta_1 - \theta_2$ (respectively proportional to normal variables φ_- and φ_+) calculated with the numerical oscilloscope from the signals $\theta_1(t)$ and $\theta_2(t)$ delivered by the potentiometers. The two-pendulum system is initially prepared in its (symmetrical) mode $(-)$. In (a) the angular frequency Ω of the engine is set as close as possible to the Larmor angular frequency Ω_0: then $\cos\beta$ (see (52)) is approximately zero; we are at resonance and the energy transfer from mode $(-)$ to mode $(+)$ is total (the envelop of the curve labelled "$\theta_1 + \theta_2$" is pinched). In (b) the engine rotation is deliberately detuned: $\cos\beta = 0.67$; we are out of resonance and the energy transfer from mode $(-)$ to mode $(+)$ is but partial. One may notice that the maximum of the envelop curve of $\theta_1 - \theta_2$ does not coincide exactly with the waist of the envelop curve of $\theta_1 + \theta_2$, contrary to what was observed in the (very analogous) curves of figure 6 in [1]: this should be attributed to the effect of solid friction which occurs to be more effective on the time-scale $\frac{2\pi}{\Omega_{\rm eff}} = T_{\rm eff}$ of the Rabi precession than on the time-scale $\frac{2\pi}{\Omega_0} = T_0$ of the Larmor precession (since $T_{\rm eff} \gg T_0$, see conditions (50)).

Notwithstanding this perturbing effect of solid friction, it turns out to be easy to measure $T_{\rm eff}$ (time interval between two consecutive pinches of the $\theta_1 - \theta_2$ curves in figures 6). We have plotted the corresponding values of $\Omega_{\rm eff}^2$ *versus* the engine's angular frequency Ω in figure 7. The experimental points are fitted with the expected law (50*b*) (solid curve in the figure). Observe the tight resemblance with figure 7 in [1].

The minimum value of $\Omega_{\rm eff}$ is $\Omega_{\rm R}$. It is obtained at resonance ($\Omega = \Omega_0$). As expected from formula (50*b*), $\Omega_{\rm R}$ should be proportional to the length modulation depth ϵ introduced in (43*a*). We have measured $T_{\rm R} = \frac{2\pi}{\Omega_{\rm R}}$ for different values of ε and displayed the ratio $\Omega_{\rm R}/\omega_0$ as a function of ε in figure 8. According to formula (50*b*) this ratio should be equal to $\frac{\varepsilon}{4}$ (let us recall that $\sin\phi_e = 1$ in this experiment). In fact our pendula are not *simple* pendula, due to the nonzero mass of the rods and the finite extent of the cylinders. This feature has been discussed at some length in reference [2]. We shall not take this detailled discussion again here, but just give its conclusion: allowing for the caracteristics of the pendula listed in table I of [2] and for the exact formula (43*b*), the expected slope of the $\Omega_{\rm R}/\omega_0$ *versus* ε law is 0.217. The fit (solid line in figure 8) has a slope of 0.214.

We shall now use our geometrical representation of the two-pendulum's dynamics to resume the calculation carried out in the Hilbert space (see subsection 4.2).

4.4. Geometrical description of the Rabi precession

What does the Rabi precession look like in the Larmor space ? To avoid any confusion, we recall hereafter the standard answer ([10], [11]) and deliberately choose a picture slightly different from that adopted to establish equations (42): for the following discussion, we note $\{\vec{e}_X, \vec{e}_Y, \vec{e}_Z\}$ the *static* basis defined in (32*b*) in *absence* of any parametric excitation. Let us now consider the frame which rotates around axis $\vec{e}_Z$ with angular velocity $\vec{\Omega} = \Omega\vec{e}_Z$. In this frame, labelled "r", we define a static basis $\{\vec{e}_{X'}, \vec{e}_{Y'}, \vec{e}_{Z'}\}$ by:

$$\begin{aligned} \vec{e}_{X'} &= \cos\Omega t\, \vec{e}_X + \sin\Omega t\, \vec{e}_Y, \\ \vec{e}_{Y'} &= -\sin\Omega t\, \vec{e}_X + \cos\Omega t\, \vec{e}_Y, \\ \vec{e}_{Z'} &= \vec{e}_Z. \end{aligned} \tag{57}$$

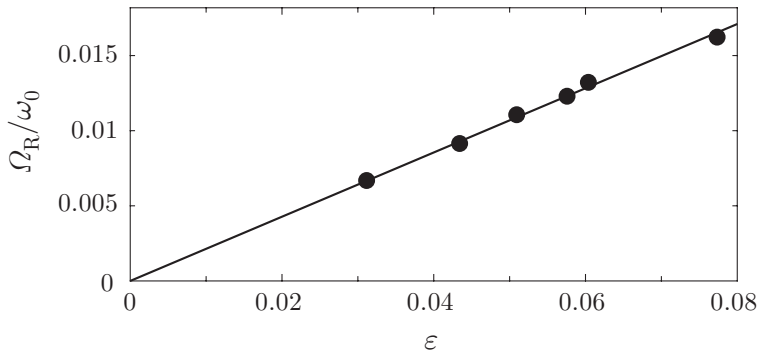

Figure 8. Influence of the length modulation depth ε on the reduced Rabi angular frequency Ω_R/ω_0. According to $(50a)$, a straight line with a slope of 0.25 is expected. Taking the fact that the pendula are not simple into account, the theoretical slope is brought down to 0.217. The fit (solid straight line) gives a slope of 0.214.

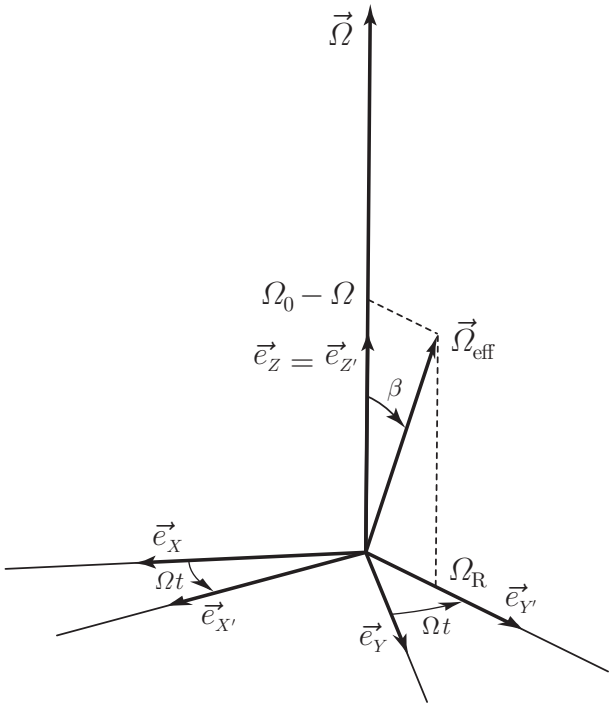

Figure 9. Effective precession angular velocity $\vec{\Omega}_{\rm eff}$ in the rotating frame with basis $\{\vec{e}_{X'}, \vec{e}_{Y'}, \vec{e}_{Z'}\}$. At resonance $\Omega = \Omega_0$, $\beta = \frac{\pi}{2}$, and $\vec{\Omega}_{\rm eff} = \Omega_{\rm R}\vec{e}_{Y'}$.

In the rotating frame, equation (34) reads:

$$\left(\frac{\mathrm{d}\vec{m}}{\mathrm{d}t}\right)_{\mathrm{r}} = \frac{\mathrm{d}\vec{m}}{\mathrm{d}t} - \vec{\Omega}\times\vec{m} = (\vec{\Omega}_0 + \delta\vec{\Omega}_0(t) - \vec{\Omega})\times\vec{m}, \tag{58}$$

where, allowing for (46), (45a), (32b), (57) and (50a):

$$\begin{aligned}\delta\vec{\Omega}_0(t) &= \delta\Delta(t)\,\vec{e}_{Z_0}\\ &= -\frac{1}{2}\omega_0\varepsilon\sin\Omega t\,(\cos\phi_e\,\vec{e}_Z + \sin\phi_e\,\vec{e}_X)\\ &= -\frac{1}{2}\omega_0\varepsilon\left[\cos\phi_e\,\sin\Omega t\,\vec{e}_{Z'} + \sin\phi_e\,(\sin\Omega t\,\cos\Omega t\,\vec{e}_{X'} - \sin^2\Omega t\,\vec{e}_{Y'})\right]\\ &= -\frac{1}{2}\omega_0\varepsilon\cos\phi_e\,\sin\Omega t\,\vec{e}_{Z'} + \Omega_{\mathrm{R}}\left[\vec{e}_{Y'} - (\sin 2\Omega t\,\vec{e}_{X'} + \cos 2\Omega t\,\vec{e}_{Y'})\right].\end{aligned} \tag{59}$$

Thus, the precession vector $\vec{\Omega}_0 + \delta\vec{\Omega}_0(t) - \vec{\Omega}$ reads, in the rotating frame, as the sum of three terms:

(i) a term parallel to $\vec{e}_{Z'}$ and *oscillating* with angular frequency Ω,

(ii) a term *rotating* around $\vec{e}_{Z'}$ with angular frequency 2Ω,

(iii) a *static* term

$$\vec{\Omega}_{\mathrm{eff}} = (\Omega_0 - \Omega)\,\vec{e}_{Z'} + \Omega_{\mathrm{R}}\,\vec{e}_{Y'}. \tag{60}$$

Provided that $\Omega_{\mathrm{eff}} \ll \Omega_0$, we can neglect the time-dependent above terms (*i.e.* the first two terms) and keep only the static one. This is in fact, once more, the SA, known under the circumstances as the "Rotating Wave Approximation" (RWA). Equation (58) is then simplified into:

$$\left(\frac{\mathrm{d}\vec{m}}{\mathrm{d}t}\right)_{\mathrm{r}} = \vec{\Omega}_{\mathrm{eff}}\times\vec{m}. \tag{61}$$

In the rotating frame, the movement of $\vec{m}$ is thus a simple precession with a constant angular frequency $\vec{\Omega}_{\mathrm{eff}}$ (see figure 9). This result justifies *a posteriori* the "Rabi precession" appellation and it provides a straightforward geometrical interpretation of formulas (54). In the static (non rotating) frame, the movement results from the combination of two rotations with respective angular velocities $\vec{\Omega}_{\mathrm{eff}}$ and $\vec{\Omega}$. Vector $\vec{m}$ is then given by

$$\vec{m}(t) = \mathrm{e}^{\vec{\Omega}t\times}\left\{\mathrm{e}^{\vec{\Omega}_{\mathrm{eff}}t\times}\,\{\vec{m}_0\}\right\} \tag{62}$$

(which, as expected, reduces to $\vec{m}(t) = \mathrm{e}^{\vec{\Omega}_0 t\times}\{\vec{m}_0\}$ in absence of parametric excitation, *i.e.* for $\Omega_{\mathrm{R}} = 0 \rightsquigarrow \vec{\Omega}_{\mathrm{eff}} = (\Omega_0 - \Omega)\,\vec{e}_Z$). The tip of vector $\vec{m}$ moves on a Bloch sphere, as shown in figures 10 in the particular case where $\vec{m}_0 = N\vec{e}_Z$ (*i.e.* the case considered in subsection 4.2 with $\alpha_-(0) = 0$ and $\alpha_+(0) = \sqrt{N}$, and yielding results (54)). In both figures 10 the representative point is initially the North pole (*i.e.* direction $+\vec{e}_Z$) of the Bloch sphere. Note by the way that analogous computed trajectories (including relaxation) can be found in the literature, *e.g.* in [12]. In figure 10a, $\Omega = \Omega_0$ (resonance): the representative point actually reaches the South pole (*i.e.* direction $-\vec{e}_Z$, representing N oscillation quanta in mode $(-)$). If $\Omega \neq \Omega_0$ (out of resonance), the $\vec{m}$-flip is not complete and the south pole of the Bloch sphere is never reached, as displayed in figure 10b.

To complete the present section 4, we would now draw up an energy balance of the above process.

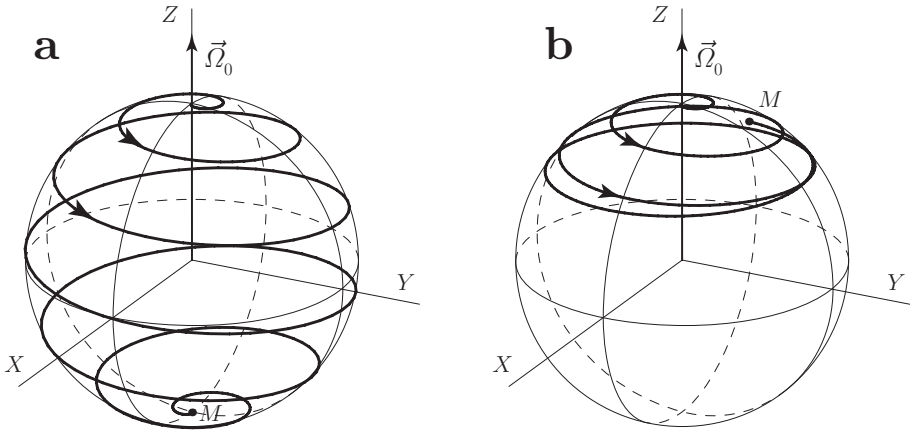

Figure 10. Trajectory of the tip M of the pseudo angular momentum $\vec{m}$ on the Bloch sphere. Departing from the North pole, point M reaches a maximum colatitude $2\min\{\beta, \pi-\beta\}$. The South pole is reached only at resonance ($\beta = \frac{\pi}{2}$) (see (a)).

4.5. Energy balance of the Rabi precession

Let T be the tension of the piano wire. When projected along pendulum 1 rods axis, Newton's Law reads:

$$M(\ddot{\ell}_1 - \ell_1\dot{\theta}_1^2) = -T + Mg\cos\theta_1. \tag{63}$$

Consequently, since $|\sin\theta_1| \ll 1$, the power $\mathcal{P}_{\rm e}$ consumed by the engine to move the cylinder along these rods is:

$$\mathcal{P}_{\rm e} = -T\dot{\ell}_1 = M\dot{\ell}_1\Big(\ddot{\ell}_1 - \ell_1\dot{\theta}_1^2 - g + g\frac{\theta_1^2}{2}\Big). \tag{64}$$

Next, averaging $\mathcal{P}_{\rm e}$ over a $\frac{2\pi}{\Omega}$ (engine rotation's period) duration, we get

$$\langle\mathcal{P}_{\rm e}\rangle = M\Big\langle\dot{\ell}_1\Big(-\ell_1\dot{\theta}_1^2 + g\frac{\theta_1^2}{2}\Big)\Big\rangle, \tag{65a}$$

or equivalently in the Glauber formalism, and deriving θ_1 and $\dot{\theta}_1$ from expression (35d) of α_1 (with $\omega_1 \simeq \omega_0$ in the quasi-degeneracy limit):

$$\langle\mathcal{P}_{\rm e}\rangle = M\frac{\hbar}{2J_1\omega_0}\Big\langle\dot{\ell}_1\Big(\ell_1\omega_0^2(\alpha_1-\alpha_1^*)^2 + \frac{g}{2}(\alpha_1+\alpha_1^*)^2\Big)\Big\rangle. \tag{65b}$$

Using (43a), neglecting the nonsecular terms α_1^2 and α_1^{*2} (which average to zero anyway), and since $M\ell_1^2 \simeq J_1$ and $g/\ell_1 \simeq \omega_0^2$, we finally have

$$\langle\mathcal{P}_{\rm e}\rangle = -\frac{\varepsilon\omega_0}{2}\hbar\Omega\langle\alpha_1\alpha_1^*\cos\Omega t\rangle. \tag{66a}$$

Since $\alpha_1\alpha_1^* = \frac{N+m_{Z_0}}{2}$, and using the basis change (32b), $\langle\mathcal{P}_{\rm e}\rangle$ reads

$$\langle\mathcal{P}_{\rm e}\rangle = -\frac{\varepsilon\omega_0}{4}\sin\phi_e\hbar\Omega\langle m_X\cos\Omega t\rangle, \tag{66b}$$

or equivalently, owing to (50a) and (57),

$$\begin{aligned}\langle\mathcal{P}_{\rm e}\rangle &= -\hbar\Omega\Omega_{\rm R}\langle(m_{X'}\cos\Omega t - m_{Y'}\sin\Omega t)\cos\Omega t\rangle \\ &= -\frac{1}{2}\hbar\Omega\Omega_{\rm R}m_{X'}(t).\end{aligned} \tag{66c}$$

Now, with the particular initial conditions considered in subsections 4.2 and 4.4, namely $\vec{m}_0 = N\vec{e}_Z$, and with definition (52) of angle β, the solution of dynamical equation (61) reads:

$$\vec{m}(t) = N\big[\sin\beta\sin\Omega_{\rm eff}t\ \vec{e}_{X'} + \sin\beta\cos\beta(1-\cos\Omega_{\rm eff}t)\ \vec{e}_{Y'} + (\cos^2\beta + \sin^2\beta\cos\Omega_{\rm eff}t)\ \vec{e}_{Z'}\big], \quad (67)$$

so that $\langle\mathcal{P}_{\rm e}\rangle$ is finally given by:

$$\langle\mathcal{P}_{\rm e}\rangle = -\frac{1}{2}N\hbar\Omega\Omega_{\rm R}\sin\beta\sin\Omega_{\rm eff}t. \quad (68)$$

As expected, this power is *negative* for the first half of the Rabi precession ($0 < t < \frac{\pi}{\Omega_{\rm eff}} = \frac{T_{\rm eff}}{2}$), which corresponds to a *stimulated emission* of energy by the two-pendulum system. The total work *received* by the engine between times $t = 0$ and $t = \frac{T_{\rm eff}}{2}$ is:

$$-\int_0^{\frac{T_{\rm eff}}{2}} {\rm d}t\ \langle\mathcal{P}_{\rm e}\rangle(t) = +N\hbar\Omega\sin^2\beta. \quad (69)$$

During the second half of the Rabi precession ($\frac{T_{\rm eff}}{2} < t < T_{\rm eff}$), power $\langle\mathcal{P}_{\rm e}\rangle$ is *positive*, which corresponds to an *absorption* of energy by the system. The total work *furnished* by the engine during this second process is $N\hbar\Omega\sin^2\beta$. At resonance ($\Omega = \Omega_0 \rightsquigarrow \sin\beta = 1$) this work is $N\hbar\Omega_0$, *i.e.* exactly the energy splitting between states $\sqrt{N}|+\rangle$ and $\sqrt{N}|-\rangle$ of our classical TLS, as required by energy conservation.

This paper is over. Let us now summarize its main results in the next section.

5. Conclusion

In this work, we have reconsidered the basic, well known and long time taught *classical* device used in our forgoing paper [1], namely two coupled harmonic oscillators, with which rather simple calculations and experiments can be performed at the undergraduate level. We have recalled what considerable simplifications can be brought in the problem as soon as both HOs are weakly coupled and have their proper angular frequencies close to each other, *i.e.* as soon as both eigenfrequencies are quasidegenerate. In this quasi-degeneracy limit, the physical state of the HO2 can be described by means of a state vector $|\psi\rangle$ belonging to some Hilbert space $\hat{\mathcal{E}}$, the time-evolution of which is easily checked to be unitary and to obey a time-independent Schrödinger-like equation of motion. Space $\hat{\mathcal{E}}$ being of dimension 2, the latter motion is naturally paralleled with that of a half-one spin evolving in a fictitious $\mathbb{R}^3$-like space $\mathbb{L}$ in a static magnetic field (Larmor precession).

Moreover we have shown that the above recalled results still hold in the case of an *adiabatic* parametric excitation of the HO2. The time-evolution (in $\hat{\mathcal{E}}$) of the state vector $|\psi\rangle$ is then ruled by a time-dependent Schrödindger-like equation, and its representing pseudo-angular momentum $\vec{m}$ then undergoes (in $\mathbb{L}$) a time-dependent pseudo magnetic field. The particular case of a small monochromatic adiabatic parametric excitation is shown to correspond to the Rabi scheme (space $\hat{\mathcal{E}}$) or equivalently to the Nuclear Magnetic Resonance (NMR, [13]) scheme (space $\mathbb{L}$). We have presented an experimental implementation of such schemes with a simplest device, the machinery of which is perfectly transparent and intuitive. It is fascinating indeed that, with but two coupled pendula, one can introduce the concept

of quantum transition and "follow" the associated trip of $\vec{m}$'s tip on the Bloch sphere in the course of time. A wealth of related concepts can be apprehended too: spin echoes, population inversion and so on. In this respect, the energy balance presented in the Rabi precession study may be used to suggest a classical equivalent of processes like energy absorption or stimulated emission, essential to any understanding of the LASER effect for example.

There is however a price to pay for this entertaining introduction to Q.M. In so far as most of the technical machinery of the present paper relies on the use of the Glauber variables, we end up with the same conclusion as in our foregoing papers [1], [2] and [9] : these variables (and the attached formalism) would deserve a better place in undergaduate level teaching and textbooks.

Acknowledgments

We acknowledge Patrick Lepers, Maurice Gilbert and Jacques Servais for their deciding contribution in achieving the initial experimental device as well as its further modifications.

References

[1] Valentin Leroy, Jean-Claude Bacri, Thierry Hocquet, and Martin Devaud. Simulating a one-half spin with two coupled pendula: the free larmor precession. *Eur. J. Phys.*, 27:1363–1383, 2006.

[2] Valentin Leroy, Jean-Claude Bacri, Thierry Hocquet, and Martin Devaud. A hamiltonian approach of the parametric excitation. *Eur. J. Phys.*, 27:469–483, 2006.

[3] Roy J. Glauber. Coherent and incoherent states of the radiation field. *Phys. Rev.*, 131(2766-2788), 1963.

[4] Roy J. Glauber. Optical coherence and photon statistics. In *Quantum optics and electronics*. New York, Gordon and Breach, 1965.

[5] Claude Cohen-Tannoudji, Bernard Diu, and Franck Laloë. *Quantum Mechanics*. New York, John Wiley, 1977.

[6] Eugen Merzbacher. *Quantum mechanics*. John Wiley and Sons, 1998.

[7] Julian Schwinger. On angular momentum. Unpublished.

[8] L. C. Biedenharn and H. Van Dam. *Quantum Theory of Angular Momentum*, pages 229–279. Academic Press, New York, 1965.

[9] Martin Devaud, Valentin Leroy, Jean-Claude Bacri, and Thierry Hocquet. The adiabatic invariant of the n-degree-of-freedom harmonic oscillator. *Eur. J. Phys.*, 29:831–843, 2008.

[10] I.-I. Rabi, N.-F. Ramsey, and J. Schwinger. Use of rotating coordinates in magnetic resonance problems. *Rev. Mod. Phys.*, 26:167–171, 1954.

[11] M. Glass-Maujean and H.-H. Stroke. Rotating coordinates and the ramsey separated oscillating field method. *Am. J. Phys.*, 59:886–890, 1991.

[12] J.-P. Grivet. Simulation of magnetic resonance experiments. *Am. J. Phys.*, 61:1133–1139, 1993.

[13] R.-E. Norberg. Resource letter nmr-epr-1 on nuclear magnetic resonance and electron paramagnetic resonance. *Am. J. Phys.*, 33:71–75, 1965.